

# On the visibility locations for continuous curves

## Abstract

The problem of determining visibility locations (VLs) on/inside a domain bounded by a planar  $C^1$ -continuous curve (without vertices), such that entire domain is covered, is discussed in this paper. The curved boundary has been used without being approximated into lines or polygons. Initially, a few observations regarding the VLs for a curved boundary have been made. It is proposed that the set of VLs required to cover the domain be placed in a manner that the VLs and the lines connecting them form a spanning tree. Along with other observations, an algorithm has been provided which gives a near optimal number of VLs. The obtained number of VLs is then compared with a visibility disjoint set, called as witness points, to obtain a measure of the ‘nearness’ of the number of VLs to the optimum. The experiments on different curved shapes illustrate that the algorithm captures the optimal solution for many shapes and near-optimal for most others.

**Keywords:** Curved boundary, Continuous curves, Visibility Locations, Guard placements, Sensor location, Splinegon, Covering problem, Camera placement

## 1. Introduction

The problem of identifying regions of visibility within a domain (or from outside of it) has been useful in many applications such as mold design for manufacturing, inspection of models, shortest path identification, placing guards to cover an art gallery, sensor location, robot motion planning etc. In the case of mold design, the problem is posed as ‘whether the model is a two-piece, given a set of viewing directions’ [1]. Alternatively, given a model, the problem is to identify optimal parting directions that reduce the number of mold pieces [2, 3].

Viewpoint selection that covers the entire object has been used in inspection. Clearly, creating an optimal set of viewpoints (or visibility locations (VLs)) will then reduce the overall cost of inspection (see [4] for a detailed survey on this topic). In the case of shortest path identification [5], the visibility graph has been a very popular construction, which can be computed using tangents [6].

Sensor location also depends on the visibility of a feature, apart from several other factors [7]. Other applications including security, computer graphics (hidden surface removal) etc. also come under the realm of visibility region identification. For further details on the applications, see [8].

The problem of visibility locations has usually considered domain bound by a polygon (a closed shape with well-defined vertices and edges as straight lines which do not intersect except at their vertices), at times with holes, typically solved by computational geometers and termed as art-gallery problem (see [9]) and occasionally polyhedra [10, 11]. However, the problem of VLs rarely considers complex objects such as curved ones. Recently, this problem for curved polygons has been addressed in [12, 13] by replacing straight edges with curves which are either piecewise convex or piecewise concave, but not a mixture of both. In the current available literature for curved polygons, vertices are well defined.

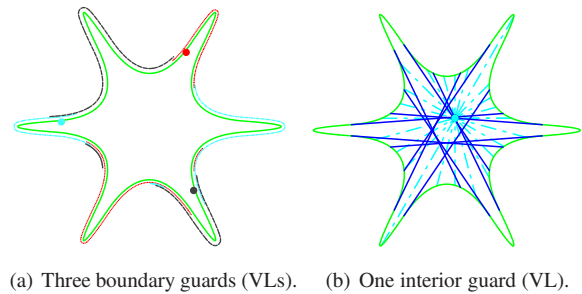


Figure 1: Boundary guards [8] vs. guard at the interior for a star-shaped domain (guards shown as dots).

Determining optimal visibility locations for a single closed continuous curved boundary (i.e without explicit notion of vertices), particularly when the locations can be interior to the domain has not been addressed, to the best of our knowledge. A conservative estimate on the number of VLs when the locations can be on the walls of the curved boundary has been provided in [8] using a visibility chart. The algorithm in [8] requires a set of candidates as input, from which either a set of VLs may be obtained or the algorithm results in failure. To aid practical solutions, they also discretize the visibility chart. Other works which discretize for practical solutions include generalised discrete framework for visibility problems in [14] and geometric multi-covering [15].

## Problem Statement, approach and the obtained results

More often than not, in practice, VLs (hereafter, termed as *guards*, for ease and clarity of explanation) are required to be placed not just on the boundary but also interior to it. For example, for a star-shaped curved polygon, as opposed to three guards on the boundary (Figure 1(a)), a single guard interior to the domain can cover it (as in Figure 1(b)). In practice, it would

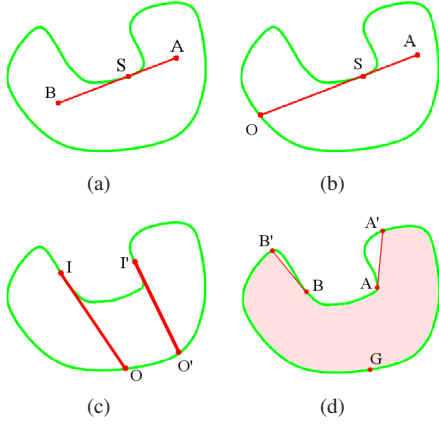


Figure 2: (a) An internal tangent AB, and (b) its silhouette and occlusion points S and O respectively. (c) Inflection points I and I', and their IPTs IO and I'O'. (d) The visibility region  $\mathcal{V}(G)$  of a guard G shown in red color.

be useful if the guards are allowed to be placed interior/on the domain (and not just on its boundary). Hence, given a planar domain bounded by a smooth (i.e. without  $C^1$  discontinuities), parametric, non-convex closed simply-connected curve  $C(t)$ , this paper aims to find the near-optimal number of guards that cover the entire domain. To the best of the knowledge of the authors, this is perhaps the first work aimed in this direction. Vertices are not explicitly defined in the curved boundary considered in this paper, and hence it is different from the curved domains considered in [12, 13]. Also, no discretization approach has been employed like in [8], though we use a rule-based approach like the one used in [16]. However, the rules have been arrived upon based on our observations. The approach presented is heuristic-based and greedy in nature. It adds one guard at a time. Moreover, we employ a first order approach to solve this problem, typically employed in hidden Markov models. It can also be noted that there can be many measures to come up with a ‘good’ guard from a candidate set (as can be seen in [16]) and our approach is based on internal tangents as it is related to the visibility in the case of a curved boundary.

We also have proposed an algorithm to compute ‘witness points’, a technique introduced in [16], based on which the optimality of the solution obtained has been conjectured to be no worse than twice the actual optimal number of guards. In practice, based on the experiments conducted, the proposed approach returns the optimal solution for many of the tested curves.

## 2. Preliminaries

Let the boundary of a domain  $\mathcal{D}$  be bounded by a parametric closed curve  $C(t)$  without  $C^1$  discontinuities. Let the exterior of the curve be denoted by  $\mathcal{D}^c$ .

### 2.1. Definitions

**Definition 1.** A point on a curve at which the curvature changes sign is called an inflection point.

**Definition 2.** A point on a curve is concave if its center of curvature and outward normal at that point are in the same direction, otherwise the point is termed convex (S in Figure 2(a) is concave, whereas O in Figure 2(b) is convex).

**Definition 3.** An internal tangent (denoted as IntT) is a line segment completely lying to the interior/on the curve (no point of the line segment lies exterior to the curve) which is a tangent to at least one point on the curve (e.g., the line segment AB in Figure 2(a) or AO in Figure 2(b)).

**Definition 4.** The point at which an internal tangent touches a curve tangentially is called its silhouette point (henceforth denoted by S) [8]. S in Figure 2(a) is the silhouette point of the IntT AB.

**Definition 5.** If an internal tangent has another point lying on the curve (apart from its silhouette point), then such a point is called an occlusion point (O in Figure 2(b)) [8], and is henceforth denoted by O.

**Definition 6.** An internal tangent starting at an inflection point is called inflection point tangent (IPT). Its starting point coincides with its silhouette point (Figure 2(c)).

**Definition 7.** A point  $P \in \mathcal{D}$  is considered visible to another point  $Q \in \mathcal{D}$ , if for all points  $x \in \overline{PQ}$ ,  $x \cap \mathcal{D}^c = \emptyset$ , i.e. no point on the line segment PQ lies completely exterior to the boundary of  $\mathcal{D}$ . Grazing contact is allowed i.e. the line segment can touch the boundary (typically tangentially).

For example, in the Figure 2(b), O is considered visible to A even though the line segment OA has a grazing contact at S.

**Definition 8.** Let  $\mathcal{V}(G) = \{x \mid x \in \mathcal{D} \text{ and } x \text{ is visible to } G\}$  be the set of points forming the visibility region of the point G (the red area in Figure 2(d) indicates the visibility region of G). A set W, consisting of points on or inside  $C(t)$  are termed as witness points [16] if visibility regions in the set are pairwise disjoint, i.e.,  $\forall_{q,r \in W} \mathcal{V}(q) \cap \mathcal{V}(r) = \emptyset$ .

### 2.2. Observations on the visibility of a guard

The motivation for our observations comes from the fact that, unlike a polygonal boundary, a  $C^1$  continuous curved boundary does not have explicitly defined vertices. A guard is assumed to be represented as a point which can see in every direction (i.e. has a  $360^\circ$  range of visibility). A set of guards is said to cover the domain if every point in the domain is visible to some guard [9]. Also, a guard cannot see through the curved boundary (i.e. the boundary is assumed to be opaque), and can either lie on or interior to it. An IntT is assumed to have at most one silhouette point. The following propositions/rules are crucial to develop an algorithm to determine the guards in a domain bound by a curved boundary. **In the subsequent sections, when we draw an internal tangent from a point, we exclude the ones that are coincident with IPTs.**

**Proposition 1.** Let  $p \in \mathcal{D} \setminus C(t)$  be a point interior to the domain.  $\mathcal{V}(p) \neq \mathcal{D}$  if and only if  $\exists$  an internal tangent which can be drawn from p.

141 *Proof.* Refer [17] (Section 2.1)  $\square$

142 Our algorithm only uses the forward direction of this dou-  
 143 ble implication, which allows us to draw internal tangents from  
 144 points which cannot guard the entire domain.

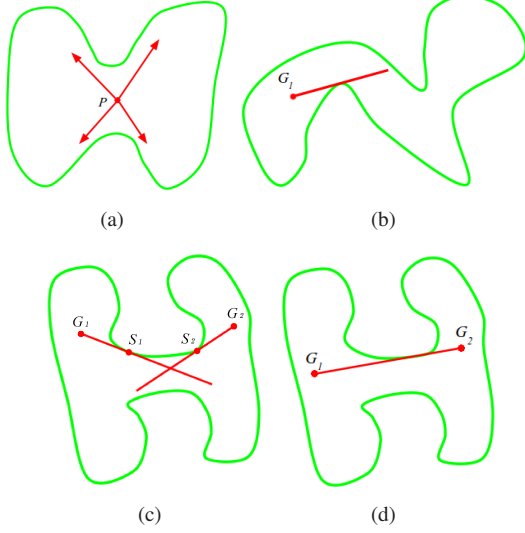


Figure 3: (a) A guard located at P has no internal tangents and covers the entire domain. (b) Even though only one IntT can be drawn from  $G_1$ , one or more guards are still required to cover the remaining region. (c) Unguarded scenario for a domain requiring two guards (d) Full coverage obtained by moving them so that one guard lies on the IntT of the other.

145 For example, in the Figure 2(b), a guard placed at A will  
 146 not see the curve portion counterclockwise from S to O due  
 147 to the presence of an internal tangent. However, in the Figure  
 148 3(a), a guard located at point P can see the entire region as no  
 149 internal tangent can be drawn from the point to the curve. For an  
 150 intricate region within a curve (Figure 3(b)), only one internal  
 151 tangent can be drawn from the guard  $G_1$ . Nevertheless,  $G_1$  is  
 152 still required to cover this region.

153 Further it can be intuitively observed that, for a curved do-  
 154 main requiring only two guards to cover it, the guards can be  
 155 placed in such a way that one guard can see the other and the  
 156 line segment connecting them is tangential to the curve. For  
 157 example, let us instead place two guards which do not see each  
 158 other (Figure 3(c)), i.e. the line joining the guards intersects the  
 159 boundary of the curve. By Proposition 1, there exists at least  
 160 one internal tangent which can be drawn from each of them.  
 161 Let the corresponding silhouette points be  $S_1$  and  $S_2$ . The re-  
 162 gion on  $C(t)$  lying between  $S_1$  and  $S_2$ , if seen clockwise, is  
 163 left unguarded. Now if these guards are moved so that their  
 164 internal tangents become collinear (i.e. by placing one guard  
 165 on the internal tangent of the other like in Figure 3(d)),  $S_1$  and  
 166  $S_2$  will coincide. As a consequence, there is no unguarded re-  
 167 gion between  $S_1$  and  $S_2$  like in the previous case. Based on this  
 168 intuition, we have the following rule:

169 **Rule 1.** Let  $G_1 \in \mathcal{D}$  be a guard which does not see the entire  
 170 domain. Another guard can be obtained by drawing an internal  
 171 tangent from  $G_1$  and choosing a point on the internal tangent  
 172 beyond its silhouette point.

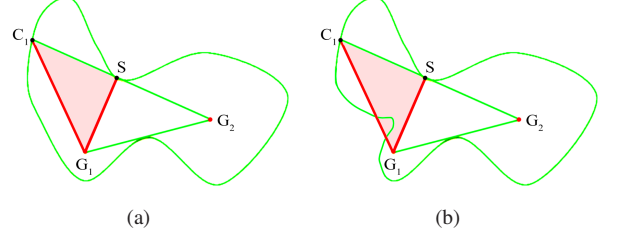


Figure 4: A figure showing two example curved domains. Guards  $G_1$  and  $G_2$  have been placed, and a new candidate guard  $C_1$  lying on the IntT drawn from  $G_2$  has been obtained. (a)  $C_1$  and  $S$  form an empty triangle with  $G_1$  (b)  $\Delta C_1 S G_1$  intersects the curved boundary.

173 Rule 1 implies that  $G_2$  in Figure 3(d), drawn as internal tan-  
 174 gent from  $G_1$ , is able to see the silhouette point of  $G_1$  and some  
 175 region beyond it. Rule 1 can be applied repeatedly to find new  
 176 guards to cover the domain. Section 4.1 later describes how to  
 177 place new guards beyond the corresponding silhouette points.  
 178 The algorithm in this paper involves the identification of one  
 179 guard as per this rule in each iteration, and hence this guard is  
 180 termed as the *subsequent guard*.

181 While Rule 1 enables us to find subsequent guards, this rule  
 182 alone is not sufficient to ensure termination of the algorithm in  
 183 all cases. This is because, in curves which require more than  
 184 one guard, every interior point has an internal tangent. Hence,  
 185 regardless of where we place our first guard, we can keep find-  
 186 ing new internal tangents (and thus new guards on them), lead-  
 187 ing to a doubling back into already guarded regions. Hence,  
 188 we add a further rule which enables us to cut down on possibly  
 189 redundant candidates for the subsequent guard. This is based  
 190 on the intuition that a subsequent guard placed on an internal  
 191 tangent of an existing guard  $G$  may not be required when the  
 192 region beyond the intT's silhouette point is already visible to  
 193 another existing guard. For example, in Figure 4(a), let  $G_1$  and  
 194  $G_2$  be the current set of guards. Let  $G_2 C_1$  be an internal tan-  
 195 gent drawn from  $G_2$  and  $C_1$  be the subsequent guard obtained  
 196 by Rule 1. Since  $S C_1$  is visible to an existing guard  $G_1$ , the  
 197 new candidate  $C_1$  is not required in this case. So we propose  
 198 the rule:

199 **Rule 2.** Empty triangle property: An internal tangent drawn  
 200 from an existing guard is considered for determining a subse-  
 201 quent guard only if the triangles formed by its silhouette point  
 202  $S$  and occlusion point  $O$  with each of the remaining guards are  
 203 not completely interior to the domain, i.e. given a set of exist-  
 204 ing guards  $\mathcal{G}$  and an intT drawn from  $G_1$ , no subsequent guards  
 205 will be placed on intT if  $\exists G_i \in \mathcal{G} \setminus G_1$  such that  $\Delta(S O G_i) \subset \mathcal{D}$ .

206 Such triangles which lie completely inside  $\mathcal{D}$  are referred  
 207 to as *empty triangles*. For example, the internal tangent  $G_2 C_1$   
 208 forms an empty triangle  $\Delta(S C_1 G_1)$  with  $G_1$  in Fig. 4(a) and  
 209 hence no guard be placed on  $G_2 C_1$ . It can be seen that  $G_1$  and  
 210  $G_2$  are sufficient to cover the domain. On the other hand, in Fig.  
 211 4(b), where  $\Delta(S C_1 G_1)$  is not an empty triangle, a guard at  $C_1$  is  
 212 needed.

213 **Definition 9.** An internal tangent from a guard is called a valid  
 214 internal tangent, and needs to be considered for determining

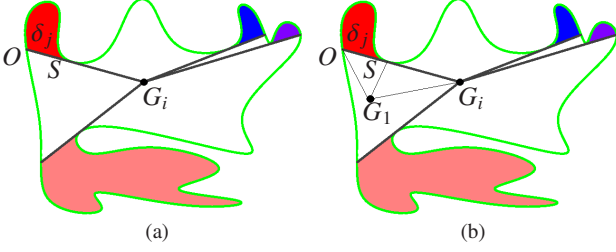


Figure 5: Proof of Proposition 2 - repeated application of Rules 1 and 2 can cover the entire domain.

subsequent guards, only if it satisfies the empty triangle property (Rule 2).

**Proposition 2.** Given a domain  $\mathcal{D}$  and an initial set of guards  $\mathcal{G}$ , repeated application of Rule 1 and Rule 2 will eventually give a new set of guards  $\mathcal{G}'$  which can cover the entire domain.

*Proof.* Assume, on the contrary, that we have a set of guards  $\mathcal{G}'$  which do not fully guard  $\mathcal{D}$  and that no subsequent guards can be added by Rule 1 because of Rule 2 (i.e. none of the existing guards have valid internal tangents). Let  $\{\delta_1, \delta_2, \dots\}$  be the set of disjoint components in  $\mathcal{D}$  that are left unguarded by  $\mathcal{G}'$  (i.e. the union of shaded regions in Figure 5(a)). The guarded portion of  $\mathcal{D}$  adjacent to any  $\delta_j$  must be guarded by some guard  $G_i \in \mathcal{G}'$  such that a part of the internal tangent  $T$  drawn from  $G_i$  to  $C(t)$  forms the boundary of  $\delta_j$  (the segment  $SO$  in Figure 5(a)). Since  $\delta_j$  is unguarded,  $T$  must have been rejected as a valid internal tangent due to Rule 2, and hence it forms an empty triangle with some guard. Let this guard be  $G_1$ , i.e. we have  $S, O \in \mathcal{V}(G_1)$ . Because the domain is simply connected, the segment  $\overline{SO} \in \mathcal{V}(G_1)$ . Since  $G_1$  can see any point on  $\overline{SO}$ , it can also see some point  $P$  lying on  $SO$  which is also a part of the boundary of  $\delta_j$ . So  $\exists P$  not lying on  $C(t)$  such that  $\overline{G_1P}$  can be extended to cross over into  $\delta_j$ . This means that a point interior to  $\delta_j$  is visible to the guard  $G_1$ , which contradicts the assumption that  $\delta_j$  is, in fact, unguarded.  $\square$

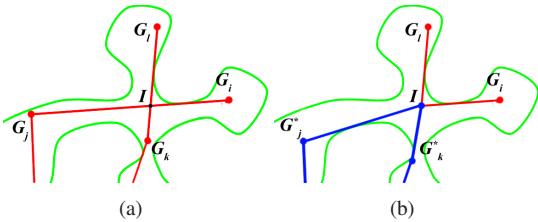


Figure 6: Corollary 1: (a) A configuration of guards such that internal tangents intersect at  $I$ , (b)  $I$  is added to the guard set, and  $G_j$  and  $G_k$  are recomputed via internal tangents from  $I$  to give a new set of guards joined by non-intersecting internal tangents.

**Corollary 1.** There exists a set of guards covering the entire domain such that every guard is connected to at least one other guard by a valid internal tangent, and the internal tangents are non-intersecting except at their end points.

*Proof.* Let us start with a set of guards which are connected by internal tangents such that some tangent  $\overline{G_iG_j}$  intersects another tangent, say  $\overline{G_kG_l}$  at the point  $I$ . Since we do not want intersections, we create a new guard at  $I$ . However, doing this means that  $I$  is not connected via an internal tangent to one of the guards from  $G_i$  and  $G_j$ , and one from  $G_k$  and  $G_l$  (segments  $IG_j$  and  $IG_k$  in Figure 6(a) are no longer internal tangents). More precisely, if the silhouette point of  $\overline{G_iG_j}$  lies on the segment  $G_iI$ ,  $G_iI$  remains an internal tangent and  $IG_j$  is no longer one, and vice versa.

This is a problem because we require the line segments joining all our guards to be internal tangents. To remedy this, we can delete such guards whose segments with  $I$  no longer form internal tangents, and their subgraphs, from the guard set. This will leave some part of the domain uncovered. Now, by Proposition 2, we have valid internal tangents which we can construct from  $I$  to place new guards ( $G_j^*$  and  $G_k^*$  in Figure 6(b)) until the domain is covered again. The empty triangle property is not broken at any point doing this construction and now have a set of guards covering the entire domain, joined by non-intersecting internal tangents.  $\square$

**Proposition 3.** Let  $\mathcal{G}$  denote a planar graph with its vertices as guards and the edges as the internal tangents between the guards as obtained by Rule 1 and Rule 2. There exists at least one set of guards forming the vertex set of  $\mathcal{G}$  that can cover the entire domain such that  $\mathcal{G}$  forms a spanning tree [18].

*Proof.* Once an initial guard is located (see Sections 4.1 and 4.2), by Rule 1, we can draw internal tangents from the existing guard, where a subsequent guard is placed on one of the internal tangents. This process can be repeated till the entire domain is covered (when there are some portions left uncovered, then there exists a valid IntT (Proposition 1 and Proposition 2) using which subsequent guards can be identified). The graph  $\mathcal{G}$  will not have a cycle because the only way of getting a cycle is by placing a subsequent guard at the same location as an existing guard, and that would contradict Rule 2 because both the silhouette and occlusion point of the new guard will be visible to the existing guard. Further, every edge in  $\mathcal{G}$  is disjoint except at its endpoints by Corollary 1. Moreover, the graph is connected as every guard has an edge to at least one another guard via an internal tangent. Hence the Proposition.  $\square$

**Proposition 4.** Let  $\mathcal{G}$  be any set of guards that can cover the entire domain  $\mathcal{D}$ . Let  $W$  be a set of visibility-disjoint witness points (refer Definition 8) in  $\mathcal{D}$ . For any  $\mathcal{G}$  and  $W$ , we will always have  $|W| \leq |\mathcal{G}|$ .

*Proof.* We will prove this by contradiction. Assume that  $\exists W \in \mathcal{D}$  such that  $|W| > |\mathcal{G}|$ . Since  $\mathcal{G}$  can see the entire domain  $\mathcal{D}$ , we have  $\forall W_i \in W, \exists G_j \in \mathcal{G}$  such that  $W_i \in \mathcal{V}(G_j)$ . But since  $|W| > |\mathcal{G}|$ , there exists at least one guard which can see two or more witness points because of the pigeonhole principle, i.e.  $\exists G_k$  such that  $\mathcal{V}(G_k)$  contains both  $W_m$  and  $W_n$  for some  $m$  and  $n$ . However, this also means that  $G_k \in \mathcal{V}(W_m)$  and  $G_k \in \mathcal{V}(W_n)$ , which means that  $\mathcal{V}(W_m) \cap \mathcal{V}(W_n) = G_k \neq \emptyset$ , which means that



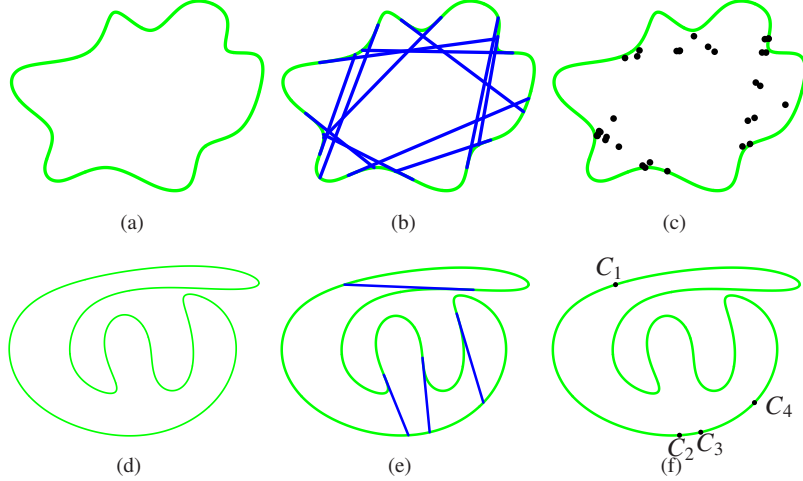


Figure 7: Demonstration of how the initial candidate guards are obtained for two test examples. (a),(d): Two  $C^1$ -continuous curves; (b),(e): IPTs drawn from each of them; (c), (f): The candidate guard set comprising of the points of intersection of IPTs with each other, or the occlusion points in case the IPTs are disjoint.

$W_m$  and  $W_n$  are not visibility-disjoint. This is a contradiction on the definition of a witness point.  $\square$

**Corollary 2.**  $|W| = |\mathcal{G}|$  implies  $\mathcal{G}$  is the minimal set of guards required to cover the domain.

As a result of this, we can say that  $W$  is a lower bound on the number of guards  $\mathcal{G}$  and can give a measure of approximately how close the value of  $|\mathcal{G}|$  is to the optimum.

### 3. Overview of the algorithm

The algorithm starts by finding a set of candidate guards derived from IPTs and their intersections (Section 4.1.1). Out of the candidate guards, one guard is chosen in each iteration based on maximum visibility (identified using the number of internal tangents from the guard) and the first order approach followed in hidden Markov models [19] (Section 4.2). Identification of internal tangents, a local-based approach has been combined with a ‘look ahead’ approach (local approaches have been shown to be working well in practise, see [16]). Though the ‘look ahead’ can be adopted at any level, in this work, we have employed to one level, termed as ‘first order’. A graph structure  $\mathcal{G}$  is initiated with the starting guard as a vertex and no edges at this juncture.

In each iteration of the algorithm, the guard among all the existing guards which has the minimum number of valid internal tangents (Definition 9) is identified (this is dealt in Section 4.3) and will henceforth be referred to as *anchor guard* for that iteration. The candidate guards for the next iteration are only chosen from points lying on the internal tangents of the anchor guard (see Section 4.1.2 for details). The subsequent guard is chosen from these candidates by using maximum visibility and the first order approach along with the empty triangle property (Section 4.2). The vertices in  $\mathcal{G}$  are updated with the identified guard and the edges are updated with the corresponding internal tangent joining the identified guard and the anchor guard. The above procedure is repeated until no valid internal tangent can

be found from any of the guards in the graph. The algorithm then terminates.

### 4. Algorithm details

The algorithm consists of the following steps:

- Finding a candidate set of guards.
- Finding a subsequent guard from the set of candidate guards.
- Picking the anchor guard from the guards in the graph.
- Termination of the algorithm.

#### 4.1. Candidate guards

##### 4.1.1. Candidate set of guards at the start

As there are no vertices in a given closed curve (Figure 7(a)), the inflection points present in the curve are used as reference. IPTs are drawn from all the inflection points till they intersect the curve at their occlusion points (Figure 7(b)). Points of intersection of the IPTs, when they intersect, and the occlusion points when they do not, are used as candidates for the first guard (Figure 7(c)). In another test example (Figure 7(d)), as all IPTs (Figure 7(e)) only intersect the curved boundary (the IPTs do not intersect among themselves), the corresponding occlusion points are chosen as candidate guards (Figure 7(f)).

##### 4.1.2. Candidate guards after identifying at least one guard

An anchor guard is chosen from the existing guards (as per Section 4.3) and only the **valid** internal tangents drawn from the anchor guard are used for finding candidates for the subsequent guard. Let  $G$  be the anchor guard and  $GO$  be an internal tangent drawn from  $G$  whose silhouette point is  $S$ . Clearly,  $G$  does not cover the entire domain because it has a valid internal tangent  $GO$ . As per Rule 1, another guard should lie somewhere on the line segment  $SO$ . Hence, we consider the occlusion point  $O$

and the points of intersection of the IPTs with the line segment  $SO$  as candidates for choosing the next guard.

For example, in the Figure 8(a), the candidates for the tangent  $GO_1$  are  $C_1$ ,  $C_2$  and  $O_1$ . In a similar manner, further candidate guards such as  $C_3$ ,  $C_4$  and  $O_2$  can be obtained from the other **valid** internal tangent  $GO_2$ , as they lie beyond its silhouette points ( $S_1$  and  $S_2$  in the Figure 8(a)) from  $G$  (do note that  $P_1$ ,  $P_2$ ,  $P_3$  and  $P_4$  have been excluded as they lie before the silhouette points). Figure 8(b) shows the set of candidate guards.

Though Proposition 1 only talks about points lying strictly interior to the domain, it holds good even when the candidate guard is a point on the boundary  $C(t)$  if the point is convex, whereas it need not be true if the point is concave (Definition 2). For example, assume that we have a domain as shown in Figure 8(c) and the guard  $G_1$  has been placed. This guard has only one **valid** internal tangent,  $G_1o$ , and since no IPT intersects with it, the only candidate guard is the occlusion point  $o$ . Placing the subsequent guard at  $o$  does not cover  $\mathcal{D}$  fully, and since one cannot draw any further internal tangent from  $o$ , the algorithm will terminate even though  $G_1$  and  $o$  do not cover the entire domain. This happens because  $o$  is concave. In practise, when a candidate guard is a concave point and no valid internal tangent can be drawn from that guard, a small perturbation towards the interior of the domain is made (such as  $o$  perturbed to  $G_2$  in Figure 8(c)) and this is added as the subsequent guard so that the algorithm does not halt prematurely.

Though there is no hard and fast rule to select a set of candidate guards, the procedure described here is similar to the one used in [16] from the algorithms  $A_2$  and  $A_{11}$  that eventually were proven to be a good candidate set. Description for determining candidate guards is shown in Algorithm 1.

---

**Algorithm 1**  $\{CG\} = \text{CandGuards}(G)$

---

**Input:** An anchor guard  $G$  (NULL at the start).

**Output:** A set of candidate guards  $\{CG\}$ .

- 1: Let  $P$  be the set of IPTs.
  - 2: **if**  $G \neq \text{NULL}$  **then**
  - 3: Find all **valid** internal tangents from  $G$ . Let the silhouette points be  $\{S\}$  and corresponding occlusion points  $\{O\}$ .
  - 4: Candidate Guards  $\{CG\} = \{O\} \cup \{P_i \cap S_j O_j\}$ ,  $\forall P_i \in P$ ,  $\forall j \neq i$
  - 5: **else**
  - 6: Candidate Guards  $\{CG\} = \{O\} \cup \{I \mid I = P_i \cap P_j \forall \{P_i, P_j\} \in P, j \neq i\}$
  - 7: **end if**
  - 8: **return**  $\{CG\}$ .
- 

#### 4.2. Selecting from the candidate guards - First order approach

Once the candidates have been obtained, one needs to choose a guard among these and update the graph  $\mathcal{G}$  accordingly. For this, the visibility of each candidate is determined by looking at internal tangents from it, as the presence of further valid internal tangents implies it cannot see part of the domain (Proposition 1). It may be noted that the candidate guards themselves are arrived at by drawing internal tangents from an anchor guard.

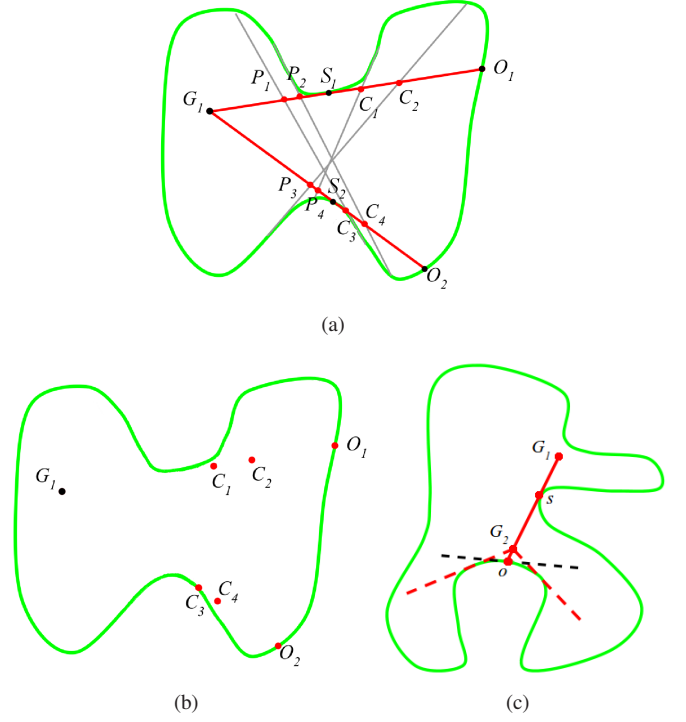


Figure 8: (a) Candidate set of guards for the given curve. The IPTs of the curve are shown in grey and the internal tangents from the existing guard  $G$  are in red, (b) The candidate guards  $C_1$ ,  $C_2$ ,  $C_3$ ,  $C_4$ ,  $O_1$  and  $O_2$  obtained as per the approach in 4.1.2. (c) Guard at concave segments.

---

**Algorithm 2**  $G = \text{SelectTheGuard}(\{CG\})$

---

**Input:** A set of candidate guards  $\{CG\}$  obtained from the anchor guard  $G_a$  ( $=\text{NULL}$  at the start).

**Output:** The chosen guard  $G^*$ .

- 1: Let  $\{CG\} = \{C_1, C_2, \dots\}$
  - 2: **for** Each guard  $C_i$  **do**
  - 3: Draw the set of internal tangents  $I$  from  $C_i$ .
  - 4: **if**  $G_a \neq \text{NULL}$  **then**
  - 5: **for** Each  $I_j$  in  $I$  **do**
  - 6: Let  $S_j$  be the silhouette point and  $O_j$  be the occlusion point.
  - 7: Let  $\mathcal{G}$  be the vertex set of  $\mathcal{G}$ .
  - 8: **if**  $\exists g \in \mathcal{G}$  such that  $\Delta(S_j O_j g) \cap C(t) = \emptyset$  **then**
  - 9:  $I = I \setminus I_j$ .
  - 10: **end if**
  - 11: **end for**
  - 12: **end if**
  - 13:  $G_1^* = \{C_i \mid C_i \text{ has minimum } |I|\}$ .
  - 14: Let  $G^*$  be a random guard from the set  $G_1^*$ .
  - 15: **end for**
  - 16:  $\mathcal{G} = \mathcal{G} \cup (G^*, I_i)$ , where  $I_i$  is the internal tangent between  $G^*$  and  $G_a$  ( $I_i$  is NULL for the starting guard).
  - 17: **return**  $G^*$ .
- 

Looking at the internal tangents from the candidate guards to choose the subsequent guard is akin to the first order approach typically followed in hidden Markov models [19]. Broadly, an  $n$ th order approach implies that the state at a predecessor level is

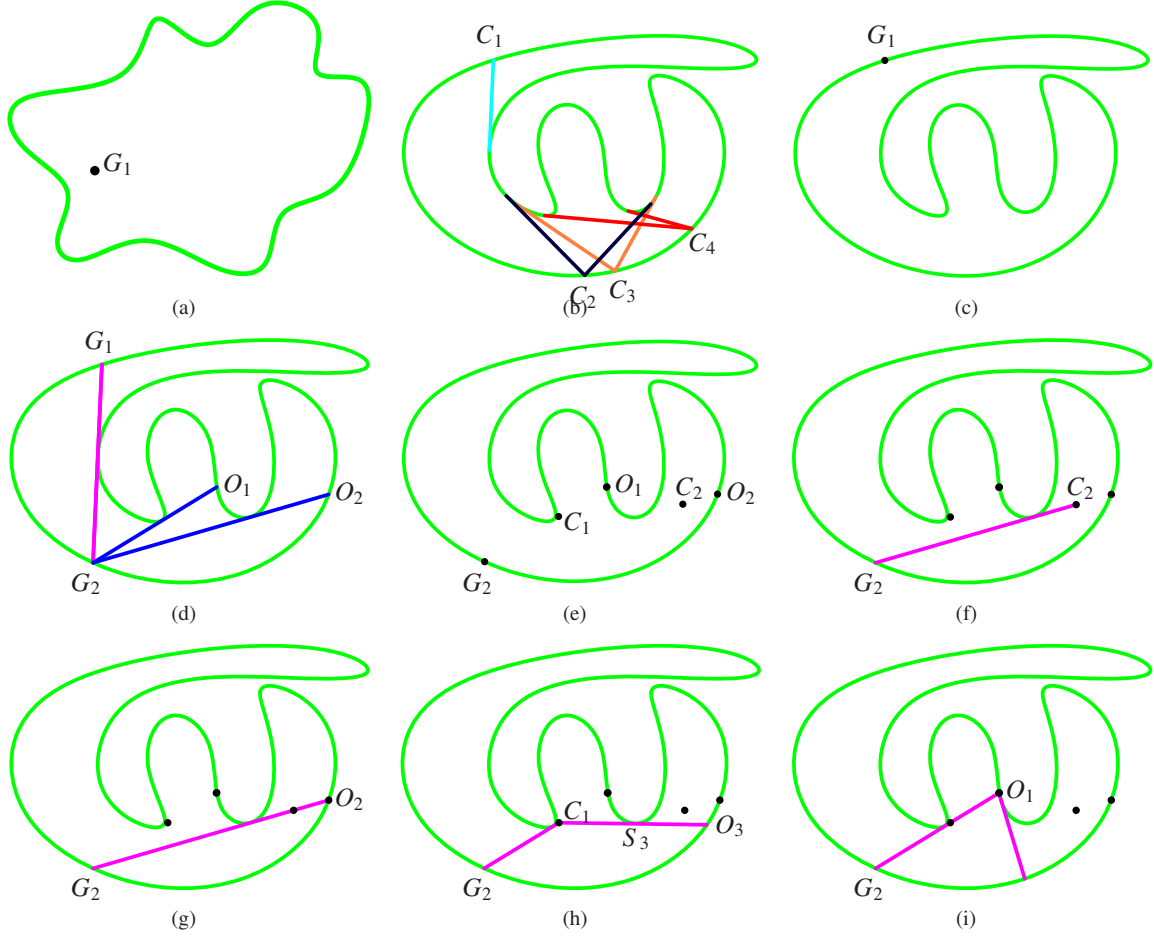


Figure 9: Illustration of choosing a guard from a set of candidate guards. (a) From the candidates in figure 7(c),  $G_1$  is chosen as a subsequent guard since it has no internal tangents (and hence it also covers the entire domain). (b)-(c) Internal tangents are drawn from the candidate points obtained in Figure 7(f) and  $G_1$ , having only one valid internal tangent, is chosen. (d)-(e) An intermediate step in the algorithm where two guards  $G_1$  and  $G_2$  have been obtained and new candidates  $C_1$ ,  $C_2$ ,  $O_1$ , and  $O_2$  are obtained taking  $G_2$  as the anchor guard. Figures (f)-(i) show the internal tangents drawn from each of these candidate guards. Since all of them form empty triangles with  $G_2$ , they have no internal tangents and any can be chosen as the subsequent guard.  $C_2$  is chosen in this case.

arrived at after a prediction made at  $n$  successive levels. If only one successive level is employed, then it is termed as first-order approach.

To select a guard from the candidate set, the number of valid internal tangents from each candidate guard is counted. Recall that a valid internal tangent should not form an ‘empty triangle’ with any of the existing guards. Note that while choosing starting guard from the candidates obtained in Section 4.1.1, the empty triangle check is redundant because no guards exist at the start. So the guard with the minimum number of internal tangents is chosen as the starting guard. For example, Figure 9(b) shows the candidate guards at the start of the algorithm and their internal tangents. All candidates but one ( $C_1$ ) have two internal tangents and hence  $C_1$  is used as the starting guard ( $G_1$  in Figures 9(c), 9(a) for the respective test examples in Figures 7(d), 7(a)) and is added to the currently empty graph  $\mathbb{G}$ .

However, when  $\mathbb{G}$  is non-empty, one needs to check for the presence of empty triangles between an internal tangent and each of the existing guards. The number of valid internal tangents (Definition 9) is counted for each candidate guard, and

the one with the minimum number is picked as the subsequent guard. The graph  $\mathbb{G}$  is then updated with this guard as a vertex and the internal tangent between the guard and its corresponding anchor guard as an edge.

For example, given the anchor guard  $G_2$ , the candidate guards are shown in Figure 9(e). Figures 9(f)-9(i) each shows internal tangents drawn from one of the four candidates. All the internal tangents form empty triangles with  $G_2$ , and hence each candidate guard has the same number of valid internal tangents, implying any of them can be chosen as the subsequent guard. For example, if  $C_2$  is selected as the guard, then  $C_2$  is added to the vertex set of  $\mathbb{G}$  and the internal tangent  $G_2C_2$  is added to the edges. Algorithm 2 encodes the procedure for selecting a guard.

#### 4.3. Picking an anchor guard

Next, an anchor guard needs to be picked among the guards currently in  $\mathbb{G}$ . This is the guard from which internal tangents will be drawn to find candidates for the next iteration. A simple procedure is used to do this. All the valid internal tangents

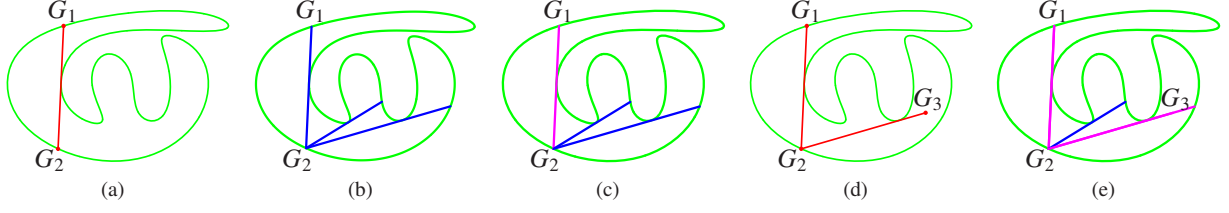


Figure 10: (a)-(c) show how an anchor guard is picked from a guard set of  $G_1$  and  $G_2$ . (a) Existing guards, (b) Internal tangents drawn from each of them (blue), (c) The tangent  $G_1G_2$  is not considered valid as it overlaps with an existing edge in  $\mathcal{G}$ . Hence,  $G_1$  has zero intTs while  $G_2$  has two.  $G_2$  is picked as the anchor guard. (d)-(e) illustrate the picking of an anchor guard after  $G_3$  is added to the guard set. (d) Guards  $G_1, G_2$  and  $G_3$  and the current graph  $\mathcal{G}$  (e) The internal tangents drawn from each of the guards (the ones which are not valid are shown in pink).  $G_2$  is picked as an anchor guard because it has least non-zero valid intTs.

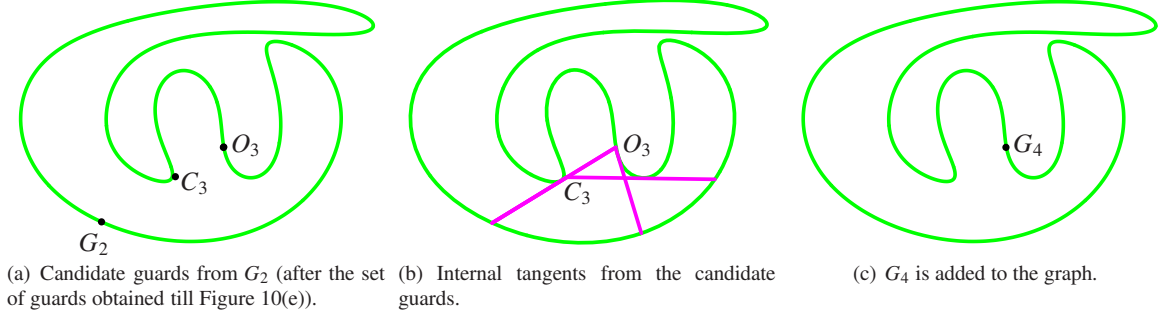


Figure 11: Finding the candidate guards from  $G_2$  and choosing the subsequent one.

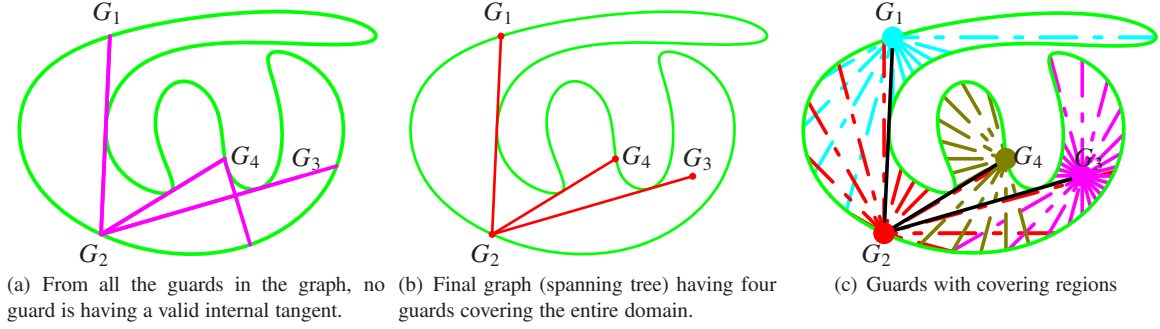


Figure 12: Termination of the algorithm.

442 from each of the guards in  $\mathcal{G}$  are found (excluding the tangents  
443 forming edges in  $\mathcal{G}$ ). The guard with the minimum number  
444 of non-zero valid internal tangents is then picked as an anchor  
445 guard.

446 Figure 10(a)-10(c) illustrate the flow for the graph consist-  
447 ing of guards  $G_1$  and  $G_2$ , where  $G_2$  gets picked as an anchor  
448 guard for finding a subsequent guard. Figure 10(d)-10(e) show  
449 another instance of the graph from which an anchor guard has  
450 to be picked for further iteration. The internal tangents which  
451 are not valid, either because of the empty triangle property or  
452 because they overlap with existing edges in the graph, are in-  
453 dicated in pink. Algorithm 3 indicates the steps in picking an  
454 anchor guard from the current graph.

#### 455 4.4. Termination of the algorithm

456 The algorithm terminates when no guard with non-zero num-  
457 ber of valid internal tangents is available as an anchor guard  
458 from the current graph, as it indicates that no internal tangents

---

#### Algorithm 3 $SG = \text{PickAnchorGuard}(\mathcal{G})$

---

**Input:** Current vertex set (guards)  $\mathcal{G}$  of  $\mathcal{G}$ .

**Output:** NULL or an anchor guard  $G_a$  from  $\mathcal{G}$ .

- 1: Let  $I_i$  be the set of valid internal tangents for each  $G_i \in \mathcal{G}$ .
  - 2: **if**  $\forall i, |I_i| == 0$  **then**
  - 3:     **return** NULL
  - 4: **else**
  - 5:     **return**  $G_a$  with minimum non-zero  $|I_i|$ .
  - 6: **end if**
- 

459 can be drawn from any of the guards in the graph, i.e. the cur-  
460 rent set of guards can see the entire domain. The termination is  
461 encapsulated in Algorithm 3 itself.

#### 462 4.5. Illustration of the algorithm

463 A high level description of the entire algorithm which re-  
464 turns the set of guards covering the domain having a curved  
465 boundary is given in Algorithm 4.



---

**Algorithm 4** FindGuards(Curved Domain  $\mathcal{D}$ )

---

```
1: Input: Domain  $\mathcal{D}$  having a continuous curved boundary.
2: Output:  $\mathcal{G}$  whose vertex set give the guards (VLs) covering  $\mathcal{D}$ .
3:  $\mathcal{G} = \{\}, i = 0$ 
4: Find the set of candidate guards,  $C\mathcal{G} = CandGuards(NULL)$ 
5: Select the guard from  $C\mathcal{G}$ ,  $G_1 = SelectTheGuard(C\mathcal{G})$ 
6: while ( $G_a = PickAnchorGuard(\bigcup_{i=1}^n G_i) \neq NULL$ ) do
7:   Find the set of candidate guards,  $C\mathcal{G} = CandGuards(G_a)$ 
8:   Select the subsequent guard,  $G_i = SelectTheGuard(C\mathcal{G})$ 
9:    $i = i + 1$ 
10: end while
11: return  $\mathcal{G}$ 
```

---

466 The illustration of the algorithm (Algorithm 4) uses the test  
467 example 2 (Figure 7(d)). The candidate guards are identified  
468 using the intersection points of the IPTs and the occlusion point  
469 of an IPT, if it does not intersect any (Figures 7(e) and 7(f)).  
470 Using the first-order approach, the starting guard ( $G_1$ ) is then  
471 identified (Figure 9(c)). Graph  $\mathcal{G}$  is initiated with the guard  $G_1$   
472 with no edges.

473 Since there is only one guard, this guard gets picked as the  
474 anchor guard for the next iteration. In the next iteration, can-  
475 didate guards are identified by internal tangents drawn from  $G_1$   
476 and using the first order approach,  $G_2$  is identified as the subse-  
477 quent guard (Figure 10(a)).  $\mathcal{G}$  is then updated with the vertex  
478  $G_2$  and the edge  $G_1G_2$ . Now, using  $PickAnchorGuard(G_1 \cup G_2)$ ,  
479 among  $G_1$  and  $G_2$ ,  $G_2$  is picked as the next anchor guard (Fig-  
480 ure 10(c)). From  $G_2$ , the set of candidate guards are identified  
481 (Figure 9(e)) and following the first order approach and per-  
482 forming checks for valid internal tangents (Figures 9(f)-9(i)),  
483 guard  $G_3$  is added to  $\mathcal{G}$  along with the internal tangent as the  
484 edge (Figure 10(d)). Then, among  $G_1$ ,  $G_2$  and  $G_3$ ,  $G_2$  is picked  
485 as the next anchor guard (Figure 10(e)). Candidate guards from  
486  $G_2$  and their further processing using first order approach is il-  
487 lustrated in Figure 11. Both  $C_3$  and  $O_3$  have no valid inter-  
488 nal tangents, so  $O_3$  is added as  $G_4$  to  $\mathcal{G}$  with the internal tan-  
489 gent between  $G_4$  and its anchor guard  $G_2$  as the edge. After  
490 this,  $PickAnchorGuard(\bigcup_{i=1}^4 G_i)$  returns NULL, as no guard has  
491 a valid internal tangent (Figure 12(a)). Hence the algorithm  
492 terminates and returns the graph  $\mathcal{G}$  (which essentially is a span-  
493 ning tree, Figure 12(b)). Figure 12(c) shows the coverage of  
494 each guard in dash-dot lines.

#### 4.6. Finding a set of witness points

496 Unlike the guard set, the witness points need to be visibility  
497 disjoint. Since we want as many witness points as possible in  
498 order to estimate a good approximation ratio, they should be  
499 placed at regions which have low visibility. Thus, inflection  
500 points, silhouette points of IntTs, and points on concave regions  
501 make for good candidates for witness points, as opposed to the

---

**Algorithm 5** FindWitnessPoints(Curved Domain  $\mathcal{D}$ )

---

```
1: Input: Domain  $\mathcal{D}$  having a continuous curved boundary.
2: Output:  $W$  consisting of witness points inside the domain  $\mathcal{D}$ .
3:  $W = \{\}, i = 0$ 
4: Find the set of inflection points  $\mathcal{I}$  of  $C(t)$ . Set the unvisited  
   inflection points  $I_{rem} = \mathcal{I}$ .
5: Find the visibility regions  $\mathcal{V}(I)$  for each inflection point by  
   finding its IPTs and IntTs.
6: while  $I_{rem} \neq NULL$  do
7:   Find the inflection point  $I^*$  which is visible to least num-  
   ber of other inflection points.
8:   Select this as a witness point,  $W = W \cup I^*$ .
9:   Update  $I_{rem} = \{I \mid I \in \mathcal{I} \text{ and } I \cap \mathcal{V}(I^*) = \emptyset\}$ 
10: end while
11: for all  $w \in W$  do
12:   Find the occlusion points of IPTs and IntTs from  $w$ , and  
   draw IntTs from each of them.
13:   Look for silhouette points  $s$  such that  $\mathcal{V}(s) \cap \mathcal{V}(W) = \emptyset$   
   and add  $s$  to  $W$ .
14: end for
15: return  $W$ 
```

---

502 occlusion points of IPTs and points lying interior to the domain  
503 (which are good candidates for finding the guards).

504 Algorithm 5 describes the steps required for finding witness  
505 points. A candidate-based first order approach is used wherein  
506 the inflection point whose visibility regions intersect with the  
507 least number of other inflection points is chosen as the starting  
508 witness point. A set of ‘unvisited inflection points’,  $I_{rem}$ , con-  
509 taining the inflection points which are visibility disjoint with  
510 every point in the witness set is maintained. This set serves as  
511 the candidate set for finding new witness points. In each step,  
512 the point which can see least number of points in  $I_{rem}$  is chosen  
513 as a witness point and the inflection points visible to it are re-  
514 moved from  $I_{rem}$ . The process iterates until all inflection points  
515 are visited, i.e. until  $I_{rem}$  becomes a null set.

516 It can be noted that the witness points in the above proce-  
517 dure have been obtained solely from inflection points. Hence,  
518 this will not give a good estimate in the case of curves having  
519 long spiral regions without inflection points. In order to ac-  
520 count for these regions, internal tangents are drawn from the  
521 occlusion points of the IPTs and IntTs of each witness point. If  
522 any silhouette points of these IPTs and IntTs is also visibility  
523 disjoint from the existing witness points, it is added to the set  
524 of witness points.

## 5. Results

526 The developed algorithm has been implemented using the  
527 IRIT geometric kernel [20], which contains function for the  
528 computation of internal tangents, and inflection, silhouette and  
529 occlusion points (for further details on such computations, please  
530 refer [8]). The curves used are represented using non uniform  
531 rational B-spline (NURBS) for the purpose of implementation,  
532 though the algorithm itself has no such restriction.



Figure 13: Results: Guards (shown in red dots), spanning tree (red dots with red lines), witness points (dots in dark blue).

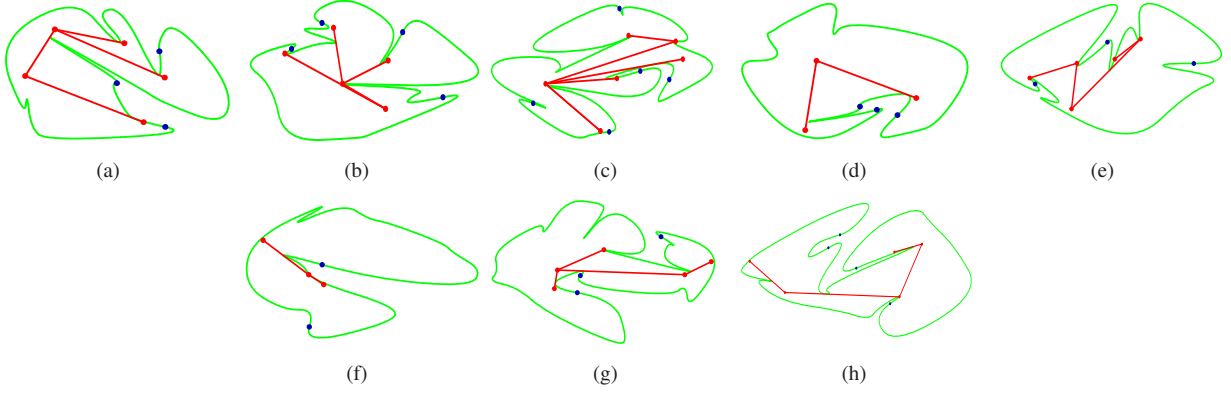


Figure 14: Results: Guards (shown in red dots), spanning tree (red dots with red lines), witness points (dots in dark blue) for random shapes.

Fig. no.	13(a)	13(b)	13(c)	13(d)	13(e)	13(f)	13(g)	13(h)	13(i)	13(j)	13(k)	13(l)	13(m)	13(n)	13(o)	13(p)	13(q)	13(r)
NOG	1	2	3	5	2	2	3	2	2	4	3	4	4	5	6	6	4	6
WP	1	2	3	4	2	2	3	2	2	3	2	3	4	5	4	5	2	4
AR	1	1	1	1.25	1	1	1	1	1	1.33	1.5	1.33	1	1	1.5	1.2	2	1.5
Time(s)	4.11	4.47	3.49	5.5	3.9	7.98	5.01	8.88	4.7	4.02	7.53	8.4	5	8.54	8.88	8.85	7.54	7.5

Table 1: The number of guards (NOG), number of witness points (WP) for various curved shapes, AR (= NOG/WP) - Approximation ratio and Running Times (in seconds) for curves in Figure 13.

Fig. no.	14(a)	14(b)	14(c)	14(d)	14(e)	14(f)	14(g)	14(h)
NOG	5	5	6	3	5	3	5	5
WP	3	4	5	3	3	2	3	4
AR	1.67	1.25	1.2	1	1.67	1.5	1.67	1.25
Time(s)	7.98	11.17	18.95	5.57	10.18	5.73	11.59	14.8

Table 2: The number of guards (NOG), number of witness points (WP) for randomly generated curved shapes, AR (= NOG/WP) - Approximation ratio and Running Times (in seconds) for curves in Figure 14.

Implementation results in Figure 13 indicate that the algorithm can handle a wide variety of curves, right from curves having a large number of inflection points to those having very few. The tested shapes include typical used ones in visibility location problems such as star-shapes, comb-like objects, spirals etc. In general, depending on the characteristics of the shape, we can either have a larger number of guards than the number of inflection points, or vice versa. For example, locally spiral-shaped objects (Figure 13(d)) have fewer inflection points but require more number of guards. This scenario has been captured by the algorithm (also see Figure 13(m) - 13(p)). On the other hand, star-shaped objects that have larger number of inflection points might require only one guard (Figure 13(a)). This has also been captured. Results for comb-like shapes are shown in Figures 13(b) and 13(c). Results for a combination of high curvature thinner and thicker regions are shown in Figures 13(e) - 13(g). The algorithm has also produced guards for objects that have low curvature regions in conjunction with higher ones in Figures 13(i) and 13(l). Guards for an object with a constricted passage is shown in Figure 13(k). The algorithm can also handle high curvature regions having different widths (Figure 13(c)). The algorithm also captures scenarios where all the guards may lie interior to the curved boundary (Figure 13(i), 13(q) and 13(r)). A few more results for randomly shaped curves having very sharp turns is shown in Figure 14. These results show that the algorithm can generate guards for differently configured curves. In both Figures 13 and 14, the outputs demonstrate that the guards form a spanning tree.

## 5.1. Discussion

### 5.1.1. On the optimal number of guards

Let  $N_g$  be the number of guards returned by our algorithm. Let  $|W_p|$  be the maximum cardinality visibility independent set (i.e., maximum number of witness points that one can determine for a given curve). Then the ratio  $N_g/|W_p|$  can be said to estimate how close our algorithm's output is to the likely optimum [16]. Let this ratio be termed as approximation ratio (AR). Tables 1 and 2 show the number of guards, witness points and AR for the set of input curves in Figures 13 and 14 respectively. In many of the inputs, the obtained AR was 1, indicating the corresponding  $N_g$  is optimal (Corollary 2). In few of the cases, the AR was 1.5 and in others, between 1 and 1.67. In the worst case, the AR obtained was 2 (Figure 13(q)). Another point worth noting is that the maximum number of witness points need not always be equal to the minimum number of guards (e.g. in Figure 13(q), there is no way of placing three or more witness points whose visibility regions do not intersect),

i.e.  $W_p$  is not necessarily a 'tight' lower bound in all cases and at times, it may be less than the optimal number of guards. This might hence lead to a higher apparent approximation ratio than is actually the case. The algorithm has been tested on many cases such as star-shaped, coil-like, comb-like etc. typically used as worst-case scenarios in the visibility location problems. Based on the testing for a number of curves (other than the results shown in Figures 13 and 14) and to be on the safer side, we can clearly say that the  $N_g$  is not more than twice the optimal number and hence the following conjecture:

**Conjecture 1.** *For a given curved boundary,  $N_g \leq 2N_{op}$ , where  $N_{op}$  is the optimal number of guards.*

### 5.1.2. Comparison

To the best of our knowledge, no algorithm seems to exist for the visibility location problem for a domain having a curved boundary with no explicit vertices. Placing the guard on the curved boundary has been addressed in [8] using a discretized approach with an exhaustive search and gives a conservative estimate (not optimal). Perhaps, we use only a subset of computations as that of [8]. We believe that our approach of using internal tangents characterizes the local shape and geometry of the domain well. Framework for visibility problems in [14] also use a discretization-based approach whereas the approach provided in [15], apart from discretization, also uses one hundred guards as the initial set. Running time of the results on an intel core i5, 2.80GHz with a 4GB RAM are of the order of a few seconds, as indicated in Tables 1 and 2 (the running times of other works cannot be compared directly as the configurations are different from those in this paper). As our running times are not too slow, it is a reasonable trade off with discretization, which introduces gaps in visibility maps and hence not guaranteeing 100% coverage [14] as opposed to 100% coverage as can be seen from the results in Figures 13 and 14. It can be noted that, in [8], the running times are of the order of a few seconds to over a minute on a modern PC. As our starting candidate guards include intersection of IPTs, our algorithm has the ability to capture domains that are guarded by a single guard, which is not possible to achieve if the guards are only on the boundary (such as [8]), see Figure 1.

Other literatures related to curved boundary such as [12, 13] use the explicit notion of vertices. It is not possible to compare with their results even after artificially adding vertices at inflection points and splitting the curve boundary into concave and convex segments. This is because [12] only considers polygons with edges which are either *all* piecewise convex or *all* piecewise concave, and [13] is only restricted to curves where the

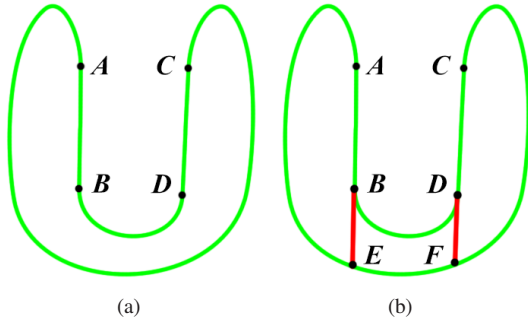


Figure 15: (a) An example where straight line segments may lead to absence of inflection points; (b) A possible fix by adding the tangents at the endpoints of the straight line sections, if interior to  $C(t)$ , to the list of IPTs ( $BE$  and  $DF$ ).

edges between any two vertices are convex.

### 5.1.3. Limitations

One limitation of this algorithm is that the number of candidate guards could be very large at the start, even though the curve might finally require only a single guard. For example, Figure 7(c) has a few candidate guards at the start, where as only one guard is required to cover the entire domain (Figure 13(a)). Also, ties obtained when multiple candidates have the same number of valid internal tangents are currently broken randomly. A better method of breaking ties remains to be found. The input curves are assumed to be  $C^1$ -continuous and hence algorithm does not handle curves with discontinuities. If there is a discontinuity such as a cusp, then there is no unique well-defined tangent at such a point, and hence the algorithm has to be suitably modified to handle such cases. One possible direction to explore would be adding the segments of the tangents at each cusp that lie interior to the curve to the set of existing IPTs at the start of the algorithm. Moreover, the algorithm cannot handle curves which contain straight line portions if the straight line portions begin or end at what otherwise would have been inflection points (such as segments  $AB$  and  $CD$  in Figure 15(a)). It might be possible to address this by detecting straight line segments and adding the tangents drawn at their endpoints, if interior to the curve, to the set of IPTs (see Fig 15(b)). Also, an internal tangent with more than one tangent point will introduce more than one silhouette point and we have not handled this case.

## 6. Conclusions and future work

In this paper, an algorithm for visibility locations (guards) that can be interior/on the curved boundary has been developed and implemented. It has been proposed that the guards have to form a spanning tree that provides a near-optimal number of visibility locations. Using the witness points, it has been shown that, in many of the tested cases, the algorithm results in optimal number of VLs. The results also enabled us to conjecture that the algorithm does not result in more than twice number of optimal VLs, as the approximation ratio was no more than 2. Results indicate that the algorithm is very amenable for implementation.

Future work would involve identifying ways for reducing the number of starting candidate guards. Another possible work is to employ the algorithm for a curved domain having holes (or obstacles) as well as to curved surfaces. Applications are also being looked at.

## References

- [1] H.-K. Ahn, M. de Berg, P. Bose, S.-W. Cheng, D. Halperin, J. Matoušek, O. Schwarzkopf, Separating an object from its cast, *Computer-Aided Design* 34 (8) (2002) 547 – 559. doi:http://dx.doi.org/10.1016/S0010-4485(01)00119-1.
- [2] K. Hui, S. Tan, Mould design with sweep operations a heuristic search approach, *Computer-Aided Design* 24 (2) (1992) 81 – 91. doi:10.1016/0010-4485(92)90002-R.
- [3] G. Elber, X. Chen, E. Cohen, Mold accessibility via gauss map analysis, in: *Proceedings International Conference on Shape Modeling and Applications*, 2004., 2004, pp. 263–272. doi:10.1109/SMI.2004.1314513.
- [4] W. R. Scott, G. Roth, J.-F. Rivest, View planning for automated three-dimensional object reconstruction and inspection, *ACM Comput. Surv.* 35 (1) (2003) 64–96. doi:10.1145/641865.641868.
- [5] B. R. Sundar, R. Muthuganapathy, Shortest path in a multiply-connected domain having curved boundaries, *Computer-Aided Design* 45 (3) (2013) 723 – 732. doi:http://dx.doi.org/10.1016/j.cad.2012.12.003.
- [6] J. K. Johnstone, A parametric solution to common tangents, in: *Proceedings International Conference on Shape Modeling and Applications*, 2001, pp. 240–249. doi:10.1109/SMA.2001.923395.
- [7] A. Bottino, A. Laurentini, L. Rosano, A new lower bound for evaluating the performances of sensor location algorithms, *Pattern Recognition Letters*doi:10.1016/j.patrec.2009.05.020.
- [8] G. Elber, R. Sayegh, G. Barequet, R. R. Martin, Two-dimensional visibility charts for continuous curves, *Shape Modeling and Applications*, 2005 International Conference (2005) 206–215.
- [9] J. O'Rourke, *Art Gallery Theorems and Algorithms*, The International Series of Monographs on Computer Science, Oxford University Press, New York, NY, 1987.
- [10] M. Liu, Y. shen Liu, K. Ramani, Computing global visibility maps for regions on the boundaries of polyhedra using minkowski sums, *Computer-Aided Design* 41 (9) (2009) 668 – 680. doi:http://dx.doi.org/10.1016/j.cad.2009.03.010.
- [11] M. Liu, K. Ramani, On minimal orthographic view covers for polyhedra, in: *2009 IEEE International Conference on Shape Modeling and Applications*, 2009, pp. 96–102. doi:10.1109/SMI.2009.5170169.
- [12] M. I. Karavelas, C. D. Tóth, E. P. Tsigaridas, Guarding curvilinear art galleries with vertex or point guards, *Computational Geometry* 42 (6-7) (2009) 522–535. doi:10.1016/j.comgeo.2008.11.002.
- [13] M. I. Karavelas, Guarding curvilinear art galleries with edge or mobile guards via 2-dominance of triangulation graphs, *Comput. Geom. Theory Appl.* 44 (1) (2011) 20–51. doi:10.1016/j.comgeo.2010.07.002.
- [14] N. Shragai, G. Elber, Geometric covering, *Computer-Aided Design* 45 (2) (2013) 243 – 251, *Solid and Physical Modeling 2012*. doi:http://dx.doi.org/10.1016/j.cad.2012.10.007.
- [15] R. Strauss, F. Isvoranu, G. Elber, Geometric multi-covering, *Computers & Graphics* 38 (2) (2014) 222 – 229. doi:http://dx.doi.org/10.1016/j.cag.2013.10.018.
- [16] Y. Amit, J. S. B. Mitchell, E. Packer, Locating guards for visibility coverage of polygons, *Int. J. Comput. Geometry Appl.* 20 (5) (2010) 601–630.
- [17] G. Elber, J. K. Johnstone, M.-S. Kim, J.-K. Seong, The kernel of a freeform surface and its duality with the convex hull of its tangential surface, *International Journal of Shape Modeling* 12 (2006) 129–142.
- [18] T. H. Cormen, C. Stein, R. L. Rivest, C. E. Leiserson, *Introduction to Algorithms*, 2nd Edition, McGraw-Hill Higher Education, 2001.
- [19] L. Rabiner, A tutorial on hidden markov models and selected applications in speech recognition, *Proceedings of the IEEE* 77 (2) (1989) 257–286. doi:10.1109/5.18626.
- [20] G. Elber, *IRIT 10.0 User's Manual*, The Technion—IIT, Haifa, Israel (2009).